J Mol Model (2005) 11: 1–7
DOI 10.1007/s00894-004-0202-0

ORIGINAL PAPER

Peter Politzer · Pat Lane · Jane S. Murray
Monica C. Concha

Comparative analysis of surface electrostatic potentials of carbon, boron/nitrogen and carbon/boron/nitrogen model nanotubes

Received: 18 March 2004 / Accepted: 18 August 2004 / Published online: 14 October 2004

Abstract We have extended an earlier study, in which we characterized in detail the electrostatic potentials on the inner and outer surfaces of a group of carbon and B_xN_x model nanotubes, to include several additional ones with smaller diameters plus a new category, $C_{2x}B_xN_x$. The statistical features of the surface potentials are presented and analyzed for a total of 19 tubes as well as fullerene and a small model graphene. The potentials on the surfaces of the carbon systems are relatively weak and rather bland; they are much stronger and more variable for the B_xN_x and $C_{2x}B_xN_x$. A qualitative correlation with free energies of solvation indicates that the latter two categories should have considerably greater water solubilities. The inner surfaces are generally more positive than the corresponding outer ones, while both positive and negative potentials are strengthened by increasing curvature. The outsides of B_xN_x tubes have characteristic patterns of alternating positive and negative regions, while the insides are strongly positive. In the closed $C_{2x}B_xN_x$ systems, half of the C–C bonds are double-bond-like and have negative potentials above them; the adjacent rows of boron and nitrogens show the usual B_xN_x pattern. When the $C_{2x}B_xN_x$ tubes are open, with hydrogens at the ends, the surface potentials are dominated by the B^+–H^- and N^-–H^+ linkages.

Keywords Surface electrostatic potentials · Carbon nanotubes · Boron/nitrogen nanotubes · Carbon/boron/nitrogen nanotubes

Introduction

Some potentially very important applications of nanotubes are related to the noncovalent interactions of their surfaces with gases and liquids, e.g. physical adsorption. An important factor is the large surface-to-mass ratio, which is enhanced by the fact that, in the case of a single-walled tube, *each atom* is accessible on both the inner and outer surfaces. Thus there continues to be great interest in the possible effectiveness of nanotubes as gas storage systems, focusing particularly upon hydrogen because of its promise as a "clean" fuel, [1, 2, 3, 4, 5, 6, 7, 8, 9, 10] but including other gases as well. [11, 12, 13, 14] Initial tests as pollutant traps and in separating components from liquid mixtures have already been successful. [15, 16, 17] The observation that adsorption leads to changes in electrical conductivities suggests use as chemical sensors. [18, 19, 20, 21] Catalytic functioning is being explored. [22] The initial excitement engendered by carbon nanotubes stimulated an interest in other elemental compositions, and B_xN_x [21, 23, 24, 25, 26] and various B/C/N [24, 27, 28, 29] tubes have now been prepared.

Noncovalent interactions, such as physical adsorption, [30, 31] are primarily electrostatic in nature. [31, 32, 33, 34, 35] In order to promote and more fully develop the nanotube applications mentioned above, it is essential to characterize in detail the electrostatic potentials on their surfaces. It has indeed been shown, in a series of studies that have been reviewed on several occasions, [36, 37, 38, 39] that a variety of solid, liquid and solution properties can be expressed quantitatively with good accuracy in terms of certain statistically defined features of the electrostatic potentials on the surfaces of the respective molecules. These properties include boiling points and critical constants, heats of phase transitions, solubilities and solvation free energies, partition coefficients, viscosities, diffusion coefficients, surface tensions and liquid and solid densities.

We have recently analyzed computationally the electrostatic potentials on the surfaces of a group of ten single-walled carbon and boron/nitrogen model nanotubes. [40] (This followed an analogous study of some

P. Politzer (✉) · P. Lane · J. S. Murray · M. C. Concha
Department of Chemistry, University of New Orleans,
New Orleans, LA 70148, USA
E-mail: ppolitze@uno.edu

model graphenes. [41]) In the present work we have extended the analysis to include additional types of carbon and B_xN_x nanotubes (primarily with smaller diameters) as well as a new category, $C_{2x}B_xN_x$, which is one of the C/B/N stoichiometries that has been synthesized. [27] This has brought out some interesting and rather unexpected points. We shall also address the question of the relative aqueous solvation tendencies of these systems. The solubilization of fullerene and carbon nanotubes has attracted considerable attention and the widespread current efforts to functionalize them are motivated in part by the desire to increase solubility. [42, 43, 44, 45, 46, 47, 48]

Methodology and procedure

Electrostatic potential

The electrostatic potential $V(\mathbf{r})$ that the nuclei and electrons of a system create at any point $\mathbf{r}$ is given rigorously by Eq. (1),

$$V(\mathbf{r}) = \sum_A \frac{Z_A}{|2R_{2A} - \mathbf{r}|} - \int \frac{\rho(\mathbf{r}')\mathrm{d}\mathbf{r}'}{|\mathbf{r}' - \mathbf{r}|} \tag{1}$$

in which Z_A is the charge on nucleus A, located at $\mathbf{R}_A$, and $\rho(\mathbf{r})$ is the electronic density. The sign of $V(\mathbf{r})$ in any region of space depends upon whether the contribution of the nuclei (positive) or that of the electrons (negative) is dominant there. For analyzing noncovalent interactions, we compute $V(\mathbf{r})$ on the molecular surface, or in the present context, the nanotube surface; we take this to be the 0.001 electrons/bohr^3 contour of the electronic density $\rho(\mathbf{r})$, as proposed by Bader et al. [49]

We characterize the overall pattern and specific features of the surface potential, $V_S(\mathbf{r})$, by means of certain statistical quantities:

(a) The most positive and most negative values, $V_{S,max}$ and $V_{S,min}$.

(b) The positive, negative and overall average potentials on the surface:

$$\bar{V}_S^+ = \frac{1}{n}\sum_{i=1}^{n} V_S^+(\bar{\mathbf{r}}_i) \tag{2}$$

$$\bar{V}_S^- = \frac{1}{m}\sum_{i=1}^{m} V_S^-(\mathbf{r}_i) \tag{3}$$

$$\bar{V}_S = \frac{1}{m+n}\left[\sum_{i=1}^{n} V_S^+(\mathbf{r}_i) + \sum_{i=1}^{m} V_S^-(\mathbf{r}_i)\right] \tag{4}$$

(c) The average absolute deviation of $V_S(\mathbf{r})$, Π:

$$\Pi = \frac{1}{m+n}\left[\sum_{i=1}^{m+n} |V_S(\mathbf{r}_i) - \bar{V}_S|\right] \tag{5}$$

(d) The positive, negative and total variances of $V_S(\mathbf{r})$:

$$\sigma_{tot}^2 = \sigma_+^2 + \sigma_-^2 = \frac{1}{n}\sum_{i=1}^{n}\left[V_S^+(\mathbf{r}_i) - \bar{V}_S^+\right]^2 + \frac{1}{m}\sum_{i=1}^{m}\left[V_S^-(\mathbf{r}_i) - \bar{V}_S^-\right]^2 \tag{6}$$

(e) An electrostatic balance parameter, ν:

$$\nu = \frac{\sigma_+^2\sigma_-^2}{\left[\sigma_{tot}^2\right]^2} \tag{7}$$

The locations of the maxima and minima, $V_{S,max}$ and $V_{S,min}$, correspond to sites that are favorable for the initial approaches of nucleophiles and electrophiles, respectively. Their magnitudes also correlate with hydrogen-bond-donating and -accepting tendencies. [50] The quantities defined in Eqs. (2), (3), (4), (5) and (7) are global in nature. We interpret Π as a measure of the local polarity, or internal charge separation, that is present even in systems with zero dipole moment, [51] e.g. *para*-dinitrobenzene. The variances σ_+^2, σ_-^2 and σ_{tot}^2 reflect the range and variability of $V_S(\mathbf{r})$; the contributions of the extrema are emphasized, due to the terms being squared. We introduced ν as a measure of the degree of balance between the positive and negative surface potentials; its upper limit is 0.250, when $\sigma_+^2 = \sigma_-^2$.

Systems investigated

Our initial study of nanotube surface electrostatic potentials encompassed five carbon and five B_xN_x model tubes of the following types: closed (5,5) and open (5,5), (6,1), (7,1) and (8,1). We have now expanded our treatment of single-walled carbon and B_xN_x systems to include the closed carbon (6,0), the closed and open B_xN_x (6,0), and the open B_xN_x (8,0). (Observations associated with electrostatic potentials of the open carbon (n,0) will be reported in a future publication.) For the new category that we are investigating, $C_{2x}B_xN_x$, we examined the closed (6,0) and the open (6,0), (8,0), (6,1) and (8,1). In the case of the open tubes, we followed the common practice of putting hydrogens at both ends to satisfy the unfilled valencies. [52, 53, 54, 55, 56] The stoichiometries of all of these systems are shown in Table 1.

Computational procedure

All geometries were optimized at the Hartree–Fock (HF) STO-3G level with the Gaussian 98 code. [57] HF/STO-5G electrostatic potentials were then computed on the surfaces defined by $\rho(\mathbf{r}) = 0.001$ electrons/bohr^3 and used to determine the statistical quantities discussed in the Electrostatic potential section. It is known from considerable earlier work, by us and by others, [36, 51,

Table 1 Computed surface quantities for model nanotubes, fullerene and model graphene[a,b]

System	Type	Diameter	A_S^+	A_S^-	$\bar{V}_S^+$	$\bar{V}_S^+$	Π	σ_+^2	σ_-^2	σ_{tot}^2	ν	$V_{S,max}$	$V_{S,min}$
carbon													
C_{120} (closed)[c]	(5,5)	6.9	636	80	2.6	−0.5	1.8	4.9	0.2	5.0	0.039	10.3	−1.8
$C_{80}H_{20}$[c]	(5,5)	6.9	204	462	7.0	−3.9	4.6	17.2	2.1	19.3	0.097	14.7	−8.0
C_{96} (closed)	(6,0)	5.0	490	96	3.1	−1.8	2.4	13.0	3.2	16.2	0.159	24.5	−5.9
$C_{68}H_{14}$[c]	(6,1)	5.2	201	335	6.3	−2.7	4.3	19.9	1.2	21.1	0.047	14.8	−7.4
$C_{62}H_{16}$[c]	(7,1)	6.0	180	347	7.0	−3.0	4.5	17.7	1.7	19.4	0.052	13.7	−7.3
$C_{68}H_{18}$[c]	(8,1)	6.8	194	390	7.2	−3.1	4.6	16.5	1.6	18.1	0.052	13.6	−7.3
C_{60}(fullerene)[c]			351	16	2.3	−0.5	1.7	6.5	0.1	6.5	0.015	10.7	−1.0
$C_{62}H_{20}$(graphene)[d]			200	392	6.4	−4.6	4.9	13.2	2.5	15.7	0.135	15.9	−7.9
B_xN_x													
$B_{60}N_{60}$ (closed)[c]	(5,5)	6.9	474	253	18.0	−8.3	14.0	223.4	41.7	265.1	0.133	49.0	−25.9
$B_{40}N_{40}H_{20}$[c]	(5,5)	6.9	417	261	12.3	−5.7	9.4	72.3	14.7	87.0	0.140	32.4	−14.7
$B_{48}N_{48}$ (closed)	(6,0)	5.0	374	211	17.9	−10.3	14.6	305.0	77.6	382.6	0.162	73.3	−37.1
$B_{42}N_{42}H_{12}$	(6,0)	5.0	336	270	19.3	−8.5	14.8	250.4	29.1	279.5	0.093	58.4	−26.5
$B_{40}N_{40}H_{16}$	(8,0)	6.5	370	269	18.5	−8.8	14.4	158.3	22.4	180.7	0.109	41.3	−26.9
$B_{41}N_{41}H_{14}$[c]	(6,1)	5.2	356	270	18.0	−8.2	13.9	194.5	24.9	219.4	0.101	49.8	−25.4
$B_{38}N_{38}H_{16}$[c]	(7,1)	6.0	356	260	17.5	−8.2	13.6	152.9	23.1	176.1	0.114	42.4	−23.0
$B_{42}N_{42}H_{18}$[c]	(8,1)	6.8	406	282	16.7	−8.2	13.1	126.3	23.5	149.8	0.132	37.8	−21.8
$C_{2x}B_xN_x$													
$C_{48}B_{24}N_{24}$ (closed)	(6,0)	5.0	342	253	14.7	−7.6	11.8	173.6	41.3	214.9	0.155	66.8	−30.6
$C_{42}B_{21}N_{21}H_{12}$	(6,0)	5.0	336	274	20.3	−15.3	17.9	220.0	121.3	341.3	0.229	67.8	−52.7
$C_{40}B_{20}N_{20}H_{16}$	(8,0)	6.5	369	277	18.4	−13.7	16.2	159.5	94.5	254.0	0.234	54.7	−44.4
$C_{42}B_{21}N_{21}H_{14}$	(6,1)	5.2	359	282	18.5	−13.8	16.2	172.6	87.3	259.9	0.223	58.6	−48.3
$C_{42}B_{21}N_{21}H_{18}$	(8,1)	6.8	394	294	17.4	−12.7	15.1	138.7	74.7	213.5	0.227	50.6	−42.2

[a]Units: the diameters are in Å; A_S^+ and A_S^- are in Å^2; $\bar{V}_S^+$, $\bar{V}_S^-$, Π, $V_{S,max}$ and $V_{S,min}$ are in kcal mol^{-1}; σ_+^2, σ_-^2 and σ_{tot}^2 are in (kcal mol^{-1})^2; ν is dimensionless

[b]HF/STO-5G//HF/STO-3G calculations

[c]Reference [40]

[d]Reference [41]

58, 59] that minimum basis sets are quite satisfactory for our present objectives.

Results and discussion

General

Table 1 gives the computed properties of the electrostatic potentials on the model nanotube surfaces, as well as the positive and negative areas, A_S^+ and A_S^-. For completeness, we present these data for all of the tubes studied plus fullerene, C_{60}, [40] and a model graphene [41] (with hydrogens along its peripheries).

Structures

Carbon nanotubes are frequently described as rolled-up sheets of graphene. This analogy must be qualified, however, with respect to the C–C bond length. Whereas this is uniformly 1.420 Å in graphite, [60] it can have several values in carbon nanotubes, due to differing orientations of the C–C bonds with respect to the tube axis [61, 62] plus (in the case of the closed tubes) the presence of five-membered as well as six-membered rings in the caps at the ends. [24, 63] (In the current work, the five-membered rings are arranged around a central hexagon.) The combination of five- and six-membered rings is the cause of fullerene having two distinct types of C–C bonds, for which our HF/STO-3G calculations predict lengths of 1.376 Å and 1.463 Å, [40] in satisfactory agreement with experimental determinations of 1.386–1.401 Å and 1.434–1.458 Å. [64, 65, 66] For the open tubes, another source of bond length variation is the effect of terminating them.

In our carbon model nanotubes, the computed C–C distances range primarily from 1.40 Å to 1.45 Å, thus bracketing the bond length in graphite. In contrast, the B–N bonds in the B_xN_x systems are more consistent, the great majority being 1.44 Å or 1.45 Å. The $C_{2x}B_xN_x$ present an interesting feature: About half of the C–C bonds are notably shorter than the others, 1.35 to 1.38 Å in length. This suggests that they are approaching double bond character, since the average experimental C=C distance is approximately 1.33 Å, [67] while the HF/STO-3G optimized values for the *cis* and *trans* $CH(BH_2)=CH(NH_2)$ isomers are 1.338 and 1.335 Å. The remaining C–C bonds in the $C_{2x}B_xN_x$ tubes, as well as the C–N and B–N, are mostly between 1.42 and 1.48 Å; the B–C are 1.51 Å and above.

Table 1 includes the diameters of the tubes, calculated from their estimated circumferences. [24, 63, 68] For this purpose, the average bond lengths in the carbon, B_xN_x and $C_{2x}B_xN_x$ systems were taken to be 1.44 Å, [63] 1.45 Å [68] and 1.44 Å, respectively.

Electrostatic potentials

Carbon nanotubes

In our earlier study, [40] we found that the electrostatic potentials on the particular carbon nanotube surfaces examined are, overall, quite weak and rather bland, with relatively little variability. (This applies as well to fullerene and graphene.) The addition, in the present work, of the closed (6,0) system does not significantly change this assessment. The two closed tubes that have been investigated, (5,5) C_{120} and (6,0) C_{96}, are positive over nearly their entire surfaces, both inner and outer, but only very weakly (Fig. 1); the averages, $\bar{V}_S^+$, are only 3 kcal mol^{-1} (Table 1). The inner surfaces are somewhat more positive than the outer, which we have found to be the case in all of the systems that we have examined regardless of their composition; this is presumably because the points inside are closer to more nuclei. The only negative spots on (5,5) C_{120} and (6,0) C_{96} are on the outside at the ends (caps), which are the regions of greatest curvature. This is also where, on the inside, are the most positive $V_S(\mathbf{r})$. The fact that $V_{S,max}$ is so much larger for the (6,0) tube than for the (5,5) may reflect the considerably smaller diameter of the former, which increases the curvature of both the sides and the caps.

In the case of the open carbon tubes in Table 1, the electron-donating hydrogens cause the outer carbon surfaces to become negative [40], but only very weakly, usually averaging −2 to −4 kcal mol^{-1} ($\bar{V}_S^-$) with minima $V_{S,min}$ between −7 and −8 kcal mol^{-1}; these are again on the outside near the ends. The insides of the open tubes are negative for the wider ones (but less so than the outsides), positive for the narrower. The hydrogens are the most positive portions of the open carbon tubes, with $V_{S,max}$ around 14 kcal mol^{-1}, which accounts for the increased $\bar{V}_S^+$. In general, these carbon nanotube surface potentials can be described as being characterized by weakness; their statistical properties given in Table 1 tend to be distinctly smaller in magnitude than is found for typical organic molecules (excluding alkane hydrocarbons). [38, 39, 69]

B_xN_x nanotubes

The B_xN_x surfaces are quite interesting (e.g. Fig. 2). On the lateral outsides, they all (whether closed or open) have regular patterns of positive and negative potentials associated with the boron and nitrogen atoms, respectively; these range from 15 to 25 kcal mol^{-1} and from −7 to −15 kcal mol^{-1}. The interiors are strongly positive (although less so as the diameter increases); this is where the large $V_{S,max}$ listed in Table 1 are found. The $V_{S,min}$ are usually near the ends of the tubes, reflecting the curvature in the closed ones and electron withdrawal by nitrogens from hydrogens in the open. Unlike the open carbon tubes, in which the hydrogens are always positive, they can now be either positive or negative, depending upon whether attached to a nitrogen or a boron. Figure 3 shows, as was also seen earlier, [40] that the characteristic surface pattern and strongly positive interior are maintained whether the B_xN_x tubes are closed or open with hydrogens at the ends.

As in the case of the carbon analogue, the small diameter closed (6,0) $B_{48}N_{48}$ has notably stronger and more variable positive and negative regions (Table 1). This is again due to the high degree of curvature on the sides and at the caps. The most positive regions are in the interior; the most negative are on the caps, outside.

$C_{2x}B_xN_x$ nanotubes

In proceeding to the new category, $C_{2x}B_xN_x$, we will first discuss the closed (6,0) $C_{48}B_{24}N_{24}$ (Fig. 4). Structurally, this tube is composed of three sets of rows of atoms parallel to its axis; within each set are two rows of carbons followed by two rows of alternating borons and nitrogens (Fig. 5). This sequence is repeated three times.

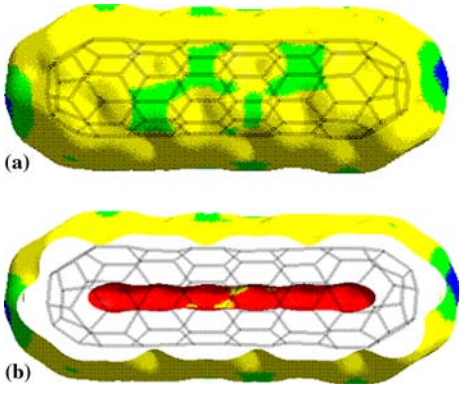

Fig. 1 Calculated electrostatic potential on the molecular surface of closed (6,0) C_{96}; **a** is an outside view, while **b** shows the interior. Color ranges, in kcal mol^{-1}: *red*, greater than 8; *yellow*, between 8 and 0; *green*, between 0 and −5; *blue*, between −5 and −7.5

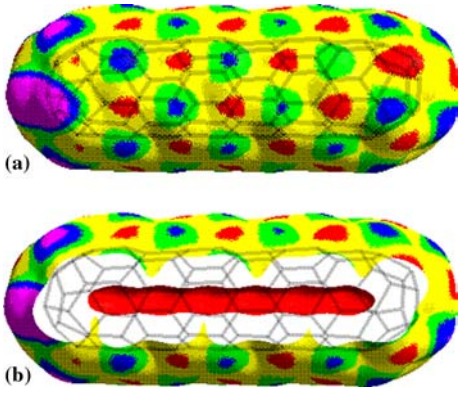

Fig. 2 Calculated electrostatic potential on the molecular surface of closed (6,0) $B_{48}N_{48}$; **a** is an outside view, while **b** shows the interior. Color ranges, in kcal mol^{-1}: *red*, greater than 20; *yellow*, between 20 and 0; *green*, between 0 and −10; *blue*, between −10 and −20; *purple*, more negative than −20

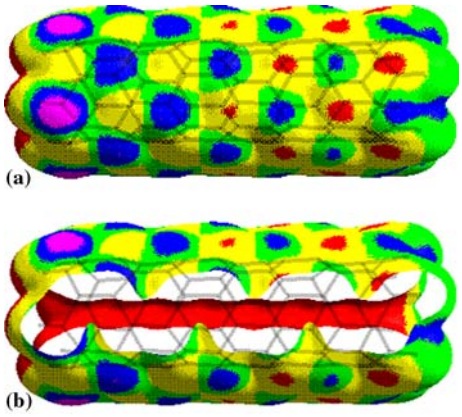

Fig. 3 Calculated electrostatic potential on the molecular surface of open (6,0) $B_{42}N_{42}H_{12}$; **a** is an outside view, while **b** shows the interior. Color ranges, in kcal mol^{-1}: *red*, greater than 20; *yellow*, between 20 and 0; *green*, between 0 and −10; *blue*, between −10 and −20; *purple*, more negative than −20

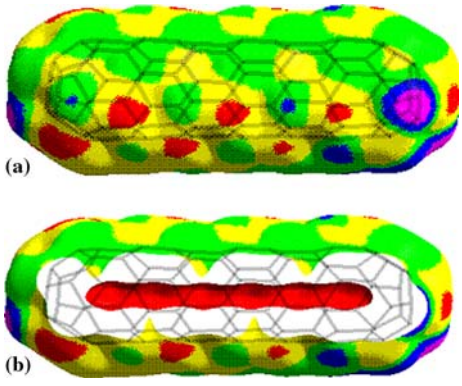

Fig. 4 Calculated electrostatic potential on the molecular surface of closed (6,0) $C_{48}B_{24}N_{24}$; **a** is an outside view, while **b** shows the interior. Color ranges, in kcal mol^{-1}: *red*, greater than 20; *yellow*, between 20 and 0; *green*, between 0 and −10; *blue*, between −10 and −20

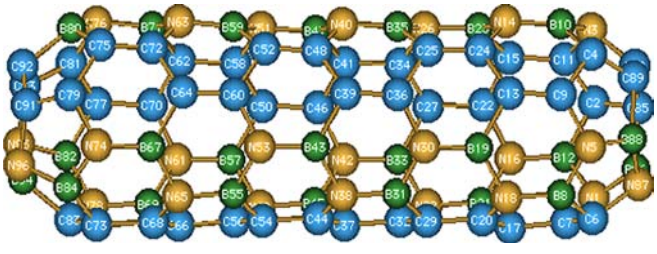

Fig. 5 Structure of closed (6,0) $C_{48}B_{24}N_{24}$

Above the borons and nitrogens are positive and negative regions, very much as in the B_xN_x systems (Fig. 2). What is different from any tube that we have seen so far, however, is the zigzag pattern of negative potentials, with magnitudes approaching −10 kcal mol^{-1}, that are associated with the rows of carbons (Fig. 4). These appear above the short C–C bonds that were mentioned in the Structures section, which are oriented parallel to the tube axis (except at the caps) and which we view as having near double bond character. This is supported by the fact that in ethylene, $H_2C=CH_2$, the $V_{S,min}$ at the HF/STO-5G level are −10.5 kcal mol^{-1} and are located above and below the midpoint of the double bond. The interior of the closed (6,0) $C_{48}B_{24}N_{24}$ is strongly positive, with $V_{S,max}$ = 66.8 kcal mol^{-1}; the $V_{S,min}$, −30.6 kcal mol^{-1}, are on the outsides of the caps, near nitrogen atoms.

The other $C_{2x}B_xN_x$ tubes in Table 1 also have the structure of two rows of carbons followed by two rows of alternating borons and nitrogens; in the (6,1) and the (8,1), however, these rows are not parallel to the axis. Unlike the B_xN_x systems, the surface potentials of these $C_{2x}B_xN_x$ model tubes are considerably affected by the presence of hydrogens at the open ends, as is shown in Figs. 6 and 7. The features that appear so distinctly for the closed (6,0) $C_{48}B_{24}N_{24}$ are no longer in evidence. In the open tubes, one end consists primarily of B–H and C–H linkages, the other of N–H and C–H. The surface potentials are dominated by the strong positive and negative regions associated with the terminal borons and nitrogens, respectively. The $V_{S,max}$ are on the inside surfaces, which are mainly positive, the $V_{S,min}$ are on the outer. Both are stronger than for the B_xN_x tubes.

Why is the effect of opening the tubes and adding hydrogens so much greater for the $C_{2x}B_xN_x$ systems than for the B_xN_x? We speculate that an important factor may be the presence, in the former, of the polarizable π electrons in the C=C double bonds.

Free energies of solvation

Some time ago, we showed that aqueous free energies of solvation can be expressed with good accuracy in terms

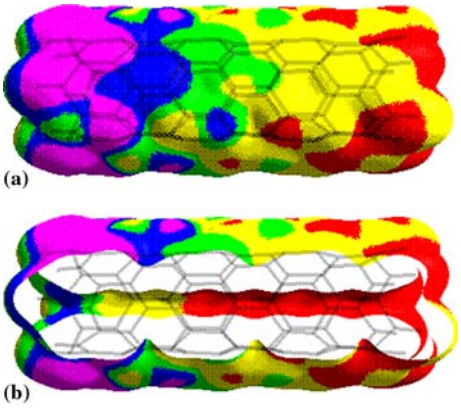

Fig. 6 Calculated electrostatic potential on the molecular surface of open (6,0) $C_{42}B_{21}N_{21}H_{12}$; **a** is an outside view, while **b** shows the interior. Color ranges, in kcal mol^{-1}: *red*, greater than 20; *yellow*, between 20 and 0; *green*, between 0 and −10; *blue*, between −10 and −20; *purple*, more negative than −20

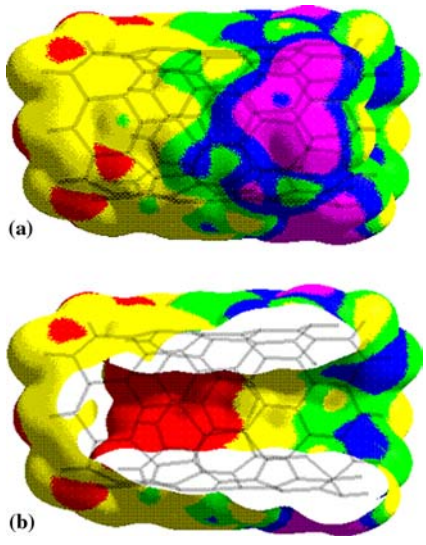

Fig. 7 Calculated electrostatic potential on the molecular surface of open (8,1) $C_{42}B_{21}N_{21}H_{18}$; **a** is an outside view, while **b** shows the interior. Color ranges, in kcal mol^{-1}: *red*, greater than 20; *yellow*, between 20 and 0; *green*, between 0 and −10; *blue*, between −10 and −20; *purple*, more negative than −20

of subsets of the statistical quantities characterizing the electrostatic potentials on the solutes' molecular surfaces. [70, 71] (These were defined in the Electrostatic potential section.) These relationships are not quantitatively applicable in the present context, because the experimental database from which they were developed (by a fitting procedure) consisted of a variety of typical organic molecular solutes, but not macrosystems such as nanotubes. They show, however, that $V_{S,max}$ plays a prominent role in determining the free energy of solvation, ΔG_{solv}, in water; ΔG_{solv} becomes more negative as $V_{S,max}$ increases. We have now found, for a series of 76 solutes, that ΔG_{solv} correlates roughly with $-V_{S,max}$ alone; the correlation coefficient is 0.81. [72] Accordingly, we suggest that $V_{S,max}$ can be used to obtain some rough qualitative insight into the relative solubilities of the respective model nanotubes. In doing this, however, we should avoid the $V_{S,max}$ due to hydrogens, since these are normally not present, as well as those inside the caps, which may not be accessible to solvents; furthermore the caps are often removed for practical applications. [1, 11, 73]

In order to eliminate the influence of hydrogens, we will focus upon the closed tubes, but looking at the $V_{S,max}$ only on their lateral surfaces, outer and inner; the $V_{S,max}$ on the caps are not considered. For the carbon tubes, the lateral $V_{S,max}$, outer and inner, are approximately 5 and 7–10 kcal mol^{-1}. For the B_xN_x and $C_{2x}B_xN_x$, they are 20–27 and 40–50 kcal mol^{-1}. Thus the $V_{S,max}$ are larger for the latter two categories by about a factor of five. While this does not translate directly into a ratio of ΔG_{solv}, it is clear that aqueous ΔG_{solv} and solubility should be considerably greater for the B_xN_x and $C_{2x}B_xN_x$ systems.

Summary

In two separate studies, we have now characterized the surface electrostatic potentials of 19 carbon, B_xN_x and $C_{2x}B_xN_x$ model nanotubes, as well as fullerene and a model graphene. Certain generalizations can be made, some of which were suggested earlier [40] but have now been reinforced.

(a) The strengths and variabilities of the inner and outer surface electrostatic potentials increase considerably in going from carbon to B_xN_x and $C_{2x}B_xN_x$. There are qualitative indications that the same is true of aqueous solubility.

(b) The inner surfaces tend to be more positive than the outer. Both positive and negative potentials are enhanced by increased curvature, such as is found at the caps or in going to tubes of smaller diameter.

(c) The outer surfaces of B_xN_x tubes have regular, stable patterns of alternating positive and negative regions. Their interiors are strongly positive. These features remain when the caps at the ends are removed and hydrogens added.

(d) In the $C_{2x}B_xN_x$ tubes, half of the C–C linkages have nearly double bond character. The outer surface of the closed (6,0) $C_{48}B_{24}N_{24}$ has zigzag paths of negative potentials above the C=C bonds adjacent to the usual B_xN_x arrangements of positive and negative regions. The inner surface is strongly positive. However, this picture is not preserved in the open tubes with hydrogens at the ends.

Overall, our results emphasize the diversity of surface electrostatic potentials, differing in patterns and in strengths, that can be achieved by varying nanotube compositions and structures. There appears to be a definite opportunity to design tubes to fulfill specific functions involving noncovalent surface interactions, e.g. trapping or sensing particular toxigens, separating components of mixtures, etc.

References

1. Dillon AC, Jones KM, Bekkedahl TA, Kiang CH, Bethune DS, Heben MJ (1997) Nature 386:377–379
2. Wang Q, Johnson JK (1999) J Phys Chem B 103:4809–4813
3. Lee SM, An KH, Lee YH, Seifert G, Frauenheim T (2001) J Am Chem Soc 123:5059–5063
4. Cheng H, Pez GR, Cooper AC (2001) J Am Chem Soc 123:5845–5846
5. Hou P, Yang Q, Bai S, Xu S, Liu M, Cheng H (2002) J Phys Chem B 106:963–966
6. Cracknell RF (2002) Mol Phys 100:2079–2086
7. Dodziuk H, Dolgonos G (2002) Chem Phys Lett 356:79–83
8. Shiraishi M, Takenobu T, Yamada A, Ata M, Kataura H (2002) Chem Phys Lett 358:213–218
9. Shiraishi M, Takenobu T, Ata M (2003) Chem Phys Lett 367:633–636
10. Zhang X, Cao D, Chen J (2003) J Phys Chem B 107:4942–4950
11. Fujiwara A, Ishii K, Suematsu H, Kataura H, Maniwa Y, Suzuki S, Achiba Y (2001) Chem Phys Lett 336:205–211

12. Yoo D-H, Rue G-H, Hwang Y-H, Kim H-K (2002) J Phys Chem B 106:3371–3374
13. Yoo D-H, Rue G-H, Chan MHW, Hwang Y-H, Kim H-K (2003) J Phys Chem B 107:1540-1542
14. Bekyarova E, Murata K, Yudasaka M, Kasuya D, Iijima S, Tanaka H, Kahoh H, Kaneko K (2003) J Phys Chem B 107:4681–4684
15. Long RW, Yang RT (2001) J Am Chem Soc 123:2058–2059
16. Mao Z, Sinnott SB (2001) J Phys Chem B 105:6916–6924
17. Peng X, Li Y, Luan Z, Di Z, Wang H, Tian B, Jia Z (2003) Chem Phys Lett 376:154–158
18. Kong J, Franklin NR, Zhou C, Chapline MG, Peng S, Cho K, Dai H (2000) Science 287:622–625
19. Collins PG, Bradley K, Ishigami M, Zettl A (2000) Science 287:1801–1804
20. Zahab A, Spina L, Poncharal P, Marliere C (2000) Phys Rev B 62:10000–10003
21. Han W-Q, Zettl A (2003) J Am Chem Soc 125:2062–2063
22. Halls MD, Schlegel HB (2002) J Phys Chem B 106:1921–1925
23. Chopra NG, Luyken RJ, Cherrey K, Crespi VH, Cohen ML, Louie SG, Zettl A (1995) Science 269:966–967
24. Harris PJF (1999) Carbon nanotubes and related structures. Cambridge University Press, Cambridge, UK
25. Tang CC, Ding XX, Huang XT, Gan ZW, Qi SR, Liu W, Fan SS (2002) Chem Phys Lett 356:254–258
26. Bae SY, Seo HW, Park J, Choi YS, Park JC, Lee SY (2003) Chem Phys Lett 374:534–541
27. Redlich Ph, Loeffler J, Ajayan PM, Bill J, Aldinger F, Ruhle M (1996) Chem Phys Lett 260:465–470
28. Golberg D, Dorozhkin P, Bando Y, Hasegawa M, Dong Z-C (2002) Chem Phys Lett 359:220–228
29. Golberg D, Bando Y, Mitome M, Kurashima K, Grobert N, Reyes-Reyes M, Terrones H, Terrones M (2002) Chem Phys Lett 360:1–7
30. Sauer J, Ugliengo P, Garrone E, Saunders VR (1994) Chem Rev 94:2095–2160
31. Naray-Szabo G, Ferenczy GG (1995) Chem Rev 95:829–847
32. Feynman RP (1939) Phys Rev 56:340–343
33. Hirschfelder JO, Curtiss CF, Bird RB (1954) Molecular theory of gases and liquids. Wiley, New York, ch 13
34. Hirschfelder JO, Meath WJ (1967) Adv Chem Phys 12:3–106
35. Buckingham AD (1967) Adv Chem Phys 12:107-142
36. Murray JS, Politzer P (1998) In: Sapse A-M (ed) Molecular orbital calculations for biological systems. Oxford University Press, New York, chapter 3
37. Murray JS, Politzer P (1998) J Mol Struct (Theochem) 425:107–114
38. Politzer P, Murray JS (1999) Trends Chem Phys 7:157–168
39. Politzer P, Murray JS (2001) Fluid Phase Equilibria 185:129–137
40. Peralta-Inga Z, Lane P, Murray JS, Boyd S, Grice ME, O'Connor CJ, Politzer P (2003) Nano Lett 3:21–28
41. Peralta-Inga Z, Murray JS, Grice ME, Boyd S, O'Connor CJ, Politzer P (2001) J Mol Struct (Theochem) 549:147–158
42. Chen RJ, Zhang Y, Wang D, Dai H (2001) J Am Chem Soc 123:3838–3839
43. Georgakilas V, Kordatos K, Prato M, Guldi DM, Holzinger M, Hirsch A (2002) J Am Chem Soc 124:760–761
44. Zhao W, Song C, Pehrsson PE (2002) J Am Chem Soc 124:12418–12419
45. Saini RK, Chiang IW, Peng H, Smalley RE, Billups WE, Hauge RH, Margrave JL (2003) J Am Chem Soc 125:3617–3621
46. Pantarotto D, Partidos CD, Graff R, Hoebeke J, Briand J-P, Prato M, Bianco A (2003) J Am Chem Soc 125:6160–6164
47. Holzinger M, Abraham J, Whelan P, Graupner R, Ley L, Hennrich F, Kappes M, Hirsch A (2003) J Am Chem Soc 125:8566–8580
48. Coleman KS, Bailey SR, Fogden S, Green MLH (2003) J Am Chem Soc 125:8722–8723
49. Bader RFW, Carroll MT, Cheeseman JR, Chang C (1987) J Am Chem Soc 109:7968–7979
50. Hagelin H, Brinck T, Berthelot M, Murray JS, Politzer P (1995) Can J Chem 73:483–488
51. Brinck T, Murray JS, Politzer P (1992) Mol Phys 76:609–617
52. Treboux G, Lapstun P, Silverbrook K (1999) Chem Phys Lett 302:60–64
53. Mazzoni MSC, Chacham H, Ordejon P, Sanchez-Portal D, Soler JM, Artacho E (1999) Phys Rev B 60:R2208-R2211
54. Liang W-Z, Wang XJ, Yokojima S, Chen G-H (2000) J Am Chem Soc 122:11129–11137
55. Bulusheva LG, Okotrub AV, Asanov IP, Fonseca A, Nagy JB (2001) J Phys Chem B 105:4853–4859
56. Bauschlicher Jr CW (2001) Nano Lett 1:223–226
57. Frisch MJ, Trucks GW, Schlegel HB, Scuseria GE, Robb MA, Cheeseman JR, Zakrezewski VG, Montgomery JA, Stratmann RE, Burant JC, Dappich S, Millam JM, Daniels AD, Kudin KN, Strain MC, Farkas O, Tomasi J, Barone V, Cossi M, Cammi R, Mennucci B, Pomelli C, Adamo C, Clifford S, Ochterski J, Petersson G, Aayala PY, Cui Q, Morokuma K, Malick DK, Rubuck AD, Raghavachari K, Foresman JB, Cioslowski J, Ortiz JV, Stefanov BB, Liu G, Liashenko A, Piskorz P, Komaromi I, Gomperts R, Martin RL, Fox D J, Keith T, Al-Laham MA, Peng CY, Nanayakkara A, Gonzalez C, Challacombe M, Gill PMW, Johnson BG, Chen W, Wong MW, Andres JL, Head-Gordon M, Replogle ES, Pople JA (1998) Gaussian 98, Revision A.5. Gaussian Inc, Pittsburgh, PA
58. Politzer P, Murray JS (1991) In: Lipkowitz KB, Boyd DB (eds) Reviews in computational chemistry, vol 2. VCH, New York, chapter 7
59. Murray JS, Brinck T, Politzer P (1992) J Mol Struct (Theochem) 255:271–281
60. Baskin Y, Meyer L (1955) Phys Rev 100:544
61. Sanchez-Portal D, Artacho E, Soler JM, Rubio A, Ordejon P (1999) Phys Rev B 59:12678–12688
62. Peralta-Inga Z, Boyd S, Murray JS, O'Connor CJ, Politzer P (2003) Struct Chem 14:431–443
63. Saito R, Dresselhaus G, Dresselhaus MS (1998) Physical properties of carbon nanotubes. Imperial College Press, London
64. Hawkins JM, Meyer A, Lewis TA, Loren S, Hollander FJ (1991) Science 252:312–313
65. Hedberg K, Hedberg L, Bethune DS, Brown CA, Dorn HC, Johnson RD, de Vries M (1991) Science 254:410–412
66. Burgi H-B, Blanc E, Schwarzenbach D, Liu S, Lu Y, Kappes MM, Ibers JA (1992) Angew Chem Int Ed Engl 31:640–643
67. Allen FH, Kennard O, Watson DG, Brammer L, Orpen AG, Taylor RJ (1987) J Chem Soc Perkin Trans II S1-S19
68. Rubio A, Corkill JL, Cohen ML (1994) Phys Rev B 49:5081–5084
69. Politzer P, Murray JS, Peralta-Inga Z (2001) Int J Quantum Chem 85:676–684
70. Murray JS, Abu-Awwad F, Politzer P (1999) J Phys Chem A 103:1853–1856
71. Politzer P, Murray JS, Abu-Awwad F (2000) Int J Quantum Chem 76:643–647
72. Murray JS, Peralta-Inga Z, Jin P, Politzer P (2004) Int J Quantum Chem (submitted)
73. Kuznetsova A, Yates Jr JT, Liu J, Smalley RE (2000) J Chem Phys 112:9590–9598